Geophysical Research Letters

RESEARCH LETTER
10.1029/2019GL084157

Multi-Centennial-Scale Variations of South American Summer Monsoon Intensity in the Southern Central Andes (24–27°S) During the Late Holocene

Sebastian T. Kock[1,2], Karsten Schittek[3], Bertil Mächtle[2], Antonio Maldonado[4,5,6], Heinz Vos[7], Liliana C. Lupo[8], Julio J. Kulemeyer[9], Holger Wissel[1], Frank Schäbitz[3], and Andreas Lücke[1]

[1]Institute of Bio- and Geosciences, Agrosphere (IBG-3), Forschungszentrum Jülich GmbH, Jülich, Germany, [2]Institute of Geography, Heidelberg Center for the Environment (HCE), Heidelberg University, Heidelberg, Germany, [3]Institute of Geography Education, University of Cologne, Cologne, Germany, [4]Centro de Estudios Avanzados en Zonas Áridas (CEAZA), La Serena, Chile, [5]Instituto de Investigación Multidisciplinar en Ciencia y Tecnología, Universidad de La Serena, La Serena, Chile, [6]Departamento de Biología Marina, Universidad Católica del Norte, Antofagasta, Chile, [7]Institute of Energy and Climate, IEK-7: Stratosphere, Forschungszentrum Jülich GmbH, Jülich, Germany, [8]Laboratorio de Palinología, Facultad de Ciencias Agrarias, Instituto de Ecorregiones Andinas (INECOA-CONICET), National University of Jujuy, Jujuy, Argentina, [9]Facultad de Ingeniería/Agrarias, Instituto de Ecorregiones Andinas (INECOA-CONICET), National University of Jujuy, Jujuy, Argentina

Key Points:
- Peat deposits from sites on the Puna Plateau about 3° latitude apart allow the development of 1,800-year-long oxygen isotope records
- Coherent fluctuations of cushion peatland oxygen isotope records reflect multi-centennial South American summer monsoon (SASM)-changes
- Differences in SASM-expression are implied by temporally changing conformity of Puna records with northern Andean SASM-reconstructions

Supporting Information:
- Supporting Information S1

Correspondence to:
S. T. Kock,
s.kock@fz-juelich.de

Citation:
Kock, S. T., Schittek, K., Mächtle, B., Maldonado, A., Vos, H., Lupo, L. C., et al. (2020). Multi-centennial-scale variations of South American summer monsoon intensity in the southern central Andes (24–27°S) during the late Holocene. *Geophysical Research Letters*, *47*, e2019GL084157. https://doi.org/10.1029/2019GL084157

Received 18 JUN 2019
Accepted 3 FEB 2020
Accepted article online 24 MAR 2018

Abstract Oxygen isotope records of cushion-plant peat cellulose from the southern central Andes capture evidence for significant environmental changes. We observe that the $\delta^{18}O_{cell}$ peatland record from Cerro Tuzgle (24°S) is in high conformity with the respective Lagunillas peatland record (27°S). During the late Holocene, two significant fluctuations occurred and are interpreted as regional moisture signals with increased precipitation amounts indicated during multi-centennial phases from 1,530 to 1,270 cal. yr BP and from 470 to 70 cal. yr BP. These fluctuations can be best explained by changes in the strength of the South American summer monsoon (SASM). This interpretation is further supported by consistency with northern Andean paleoclimate records (10–13°S) and very high correlation ($R^2 = 0.76$) with the Southern Oscillation Index. The congruent precipitation signals suggest the persistent climatic control of the SASM-strength in this latitudinal band during the last 1,800 years.

Plain Language Summary Stable oxygen isotopes ($\delta^{18}O_{cell}$) that are incorporated in cellulose of organic matter of plants accumulated by cushion peatlands on the Puna Plateau are a useful tool to investigate past environmental changes in the southern central Andes. Contemporaneous changes in the composition of $\delta^{18}O_{cell}$ became evident in the high-elevation peatlands from Cerro Tuzgle (24°S) and Lagunillas (27°S). Within the last 1,800 years, two distinct fluctuations occurred that can be interpreted as change in the regional precipitation supply which is controlled by the South American summer monsoon (SASM) intensity. According to this interpretation, specifically, high SASM-activity and, thus, increased precipitation occurred between 1,530 to 1,270 cal. yr BP and between 470 to 70 cal. yr BP whereas SASM-strength reduced before 1,530 cal. yr BP and between 1,270 to 470 cal. yr BP. Strong support for this interpretation is the high accordance with other SASM-affected paleoclimatic records of the northern central Andes (10–13°S) and high conformity with the Southern Oscillation Index. This also indicates a persistent impact of the SASM during the last 1,800 years.

1. Introduction

Located within the Arid Diagonal of South America, a region characterized by a maximum of 200 mm of annual precipitation (de Porras & Maldonado, 2016), the Puna Plateau of the southern central Andes is situated at the transition between tropical and extra-tropical atmospheric circulation systems, and thus, represents a key region for global climate dynamics. In contrast to this importance is a lack of reliable paleoclimatic data sets from this region describing Holocene climate dynamics. Recently, high-elevation cushion peatlands from the Puna have shown their potential to fill this gap (e.g., Schittek, 2014; Schittek et al., 2016).

Modern precipitation patterns on the Puna Plateau (22–27°S) are linked to changing intensities of the South American summer monsoon (SASM) system, which is sourced from the northern Tropical Atlantic and the

Amazon Basin. In the time from October to November, the onset of the SASM is initiated by a weakening of the meridional temperature gradient between tropical and subtropical latitudes, resulting in a southward displacement of the South American Low-Level-Jet (SALLJ). Connected with a southward shift of the Intertropical Convergence Zone (ITCZ) over the tropical Atlantic and Pacific, deep convection over the Amazon Basin starts to develop during austral summer from December to February (Garreaud et al., 2003; Marengo et al., 2012), which finally leads to the SALLJ-driven N-S moisture transport to the Eastern Cordillera of the Argentine Andes (Garreaud, 2000; Vera et al., 2006; Vuille et al., 2012). The Puna Plateau can additionally be affected by cold-front snowfall events occurring in response to a northward movement of cold polar air masses and cutoffs from the southern westerly circulation drifting northwards as isolated cells. Both patterns, cold-front and cutoff events, are sourced from the Pacific Ocean and linked to the Southern Hemisphere westerly wind belt (SHW) and mainly influence the western range of the extra-tropical Andes during austral winter (e.g., Vuille & Ammann, 1997). Recently, the Hadley circulation shows a poleward expansion in both hemispheres, linked to increased latitudinal movements of the ITCZ and, thus, to changes in regional precipitation patterns (Alfaro-Sánchez et al., 2018). As changes in the tropical belt also affect the SASM-intensity, it is essential to increase the knowledge about its long-term development.

The dynamics of the SASM are additionally affected by large-scale teleconnections of which one is the El Niño Southern Oscillation (ENSO). ENSO is a complex ocean-atmosphere interaction that affects the global atmospheric circulation on interannual timescales (e.g., Gergis et al., 2006). How ENSO-like oceanic and atmospheric variability interacts with large-scale climate states over decadal to centennial timescales is still not fully resolved (Henke et al., 2017). The oceanic variability of the ENSO system is closely connected to sea surface temperature anomalies of the Equatorial Pacific, while the atmospheric component, the so-called Southern Oscillation, arises as a seesaw in atmospheric mass balances between the South Pacific subtropical high and the Indonesian equatorial low (e.g., Trenberth, 1997). Long-term sea surface temperature changes, for example, in the extratropical North Pacific that are expressed in the Pacific Decadal Oscillation, can reveal other low-frequency ENSO-like modes (e.g., MacDonald & Case, 2005).

Besides a multiplicity of potential influences on the isotopic composition of precipitation like moisture source, moisture transport history, or the degree of rainout upstream (see Insel et al., 2013), evidence from observations reveal that a precipitation amount effect explains a significant fraction of $\delta^{18}O_{precipitation}$ variations in South America on seasonal and interannual time scales (The International Atomic Energy Agency/World Meteorological Organization, 2015). Instead of local condensation temperature, the primary control on the isotopic composition of precipitation in wide parts of South America is the SASM-intensity (Hardy et al., 2003; Vuille et al., 2012), establishing a negative correlation between local precipitation amount and $\delta^{18}O_{precipitation}$ signature. Numerous paleoclimatic studies in the northern central Andes (between 10 and 13°S) could thus identify changes in SASM-strength during the last 2,000 years as recorded in $\delta^{18}O$ changes of different archives (lake sediments; e.g. Bird et al., 2011), speleothems (e.g., Kanner et al., 2013), and ice cores (e.g., Thompson et al., 2013).

For the southern central Andes, a connection between $\delta^{18}O_{cellulose}$ values and moisture conditions of a cushion peatland was recently shown and related, similar as above described, to the SASM-variation (Kock, Schittek, Wissel, et al., 2019). Here, we further show that the $\delta^{18}O_{cell}$ pattern recorded in cushion peatland archives is (1) regionally uniform for the Puna Plateau between 24° and 27°S during the last 1,800 years and (2) strongly connected to centennial-scale SASM-dynamics.

2. Study Region

The Puna Plateau (22–27°S) is an endorheic plateau which represents the southern sector of the Altiplano-Puna region of the central Andes (Norini et al., 2014; Werner, 1974). Bordering the plateau to the east, the Eastern Cordillera blocks moisture originating in the Amazon Basin and the Atlantic, leading to a humidity gradient with increasing aridity towards the west. Especially in the arid west, the number of available paleoclimate archives is still considerably small. In this respect, high-Andean cushion peatlands can be valuable (paleo-)environmental recorders, especially due to their high accumulation rates that allow for chronologies up to sub-decadal resolution (e.g., Engel et al., 2014; Kock, Schittek, Mächtle, et al., 2019; Schittek et al., 2015). Further, these peatlands are very sensitive towards climatic changes and offer comparability across climatic gradients and (Schittek, 2014; Schittek et al., 2018).

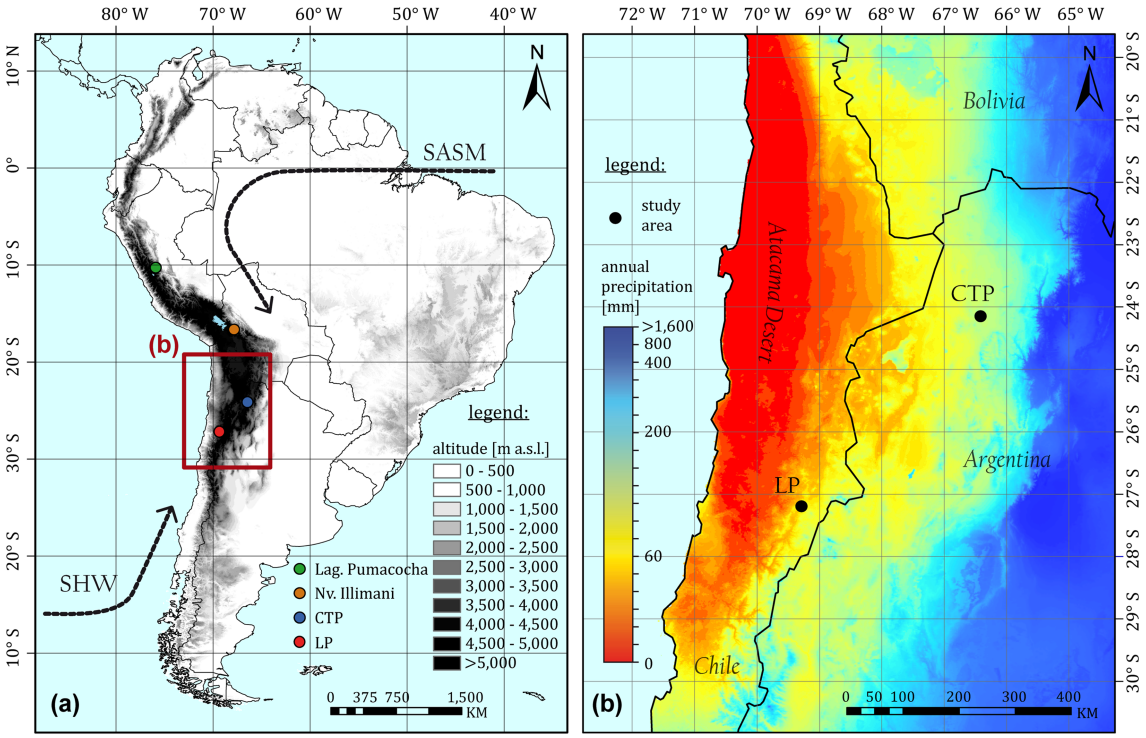

Figure 1. Study area of LP and CTP in the southern central Andes. (a) DEM of South America (data source: GTOPO30). The colored dots indicate the paleoclimate archives discussed in the text, while the marked lines represent the climatic moisture sources from the South American Summer Monsoon (SASM; low-level circulation ~925 hPa) and the Southern Hemisphere Westerlies (upper-level circulation ~300 hPa). The red square shows the position of Figure 1b. (b) Annual precipitation pattern in the study area of the southern central Andes. The black dots indicate the investigated Cerro Tuzgle peatland (CTP; 135 mm/a) and Lagunillas peatland (LP; 61 mm/a) (data source: WorldClim2 30-s precipitation data; Fick & Hijmans, 2017).

The Cerro Tuzgle peatland (CTP; 24°09′S, 66°24′W, 4,350 m a.s.l.; Kock, Schittek, Wissel, et al., 2019) and Lagunillas peatland (LP; 27°12′S, 69°17′W, 3,823 m a.s.l.; Kock, Schittek, Mächtle, et al., 2019) are both located on the Puna Plateau (Figure 1a). In contrast to the CTP record, the LP record is frequently interbedded with clastic units. While the CTP is located within a valley that features a rather protected setting from landslides with gentle slopes, LP is embedded in a common v-shaped valley with steep slopes and, thus, is exposed to repeated allochthonous sediment input. The clastic sediments of LP reflect past geomorphodynamics. They can either be related to strong, single erosional (precipitation) events with large amounts of transported sediment or to repeated, smaller erosional events with lower amounts of transported clastic material and with insufficient time to reestablish cushion plant cover (Kock, Schittek, Lücke, et al., 2019). Therefore, and contrary to CTP, the peat accumulation in LP is discontinuous, and the layers are separated by clastic units. However, both peatlands share a comparable floral composition that is dominated by the vascular plant *Oxychloe andina* with a limited number of supplementary species of the Cyperaceae family (including *Carex* and *Zameioscirpus*). Their chronologies cover the past 1,800 years with high temporal resolution (on average 10 a/cm). Under recent climatic conditions, the LP receives a distinct lower amount of precipitation compared to the CTP (Figure 1b). While the CTP receives 97% (131 of 135 mm) of annual precipitation during summer month between October and March (SASM), LP receives 61% (37 of 61 mm) within the same period (based on Fick & Hijmans, 2017). Monthly calculated $\delta^{18}O_{precipitation}$ isoscape data (Bowen, 2020; Bowen et al., 2005) of the study sites (Table S1) show most negative values occurring in February, the peak of the SASM-cycle. Taken together with regional climate station data (e.g., Mina Concordia (see Kock, Schittek, Wissel, et al., 2019), this suggests that seasonal precipitation amount and isotopic composition are linked locally, equivalent to the oxygen isotope-precipitation amount effect derived from Global Network of Isotopes in Precipitation station data (The International Atomic Energy Agency/World Meteorological Organization, 2015).

3. Materials and Methods

3.1. Age Control and Cellulose Extraction

Master core halves from LP and CTP were cut into 1-cm slices and sampled for radiocarbon dating and cellulose extraction. Bulk peat samples were used for radiocarbon dating by Accelerator Mass Spectrometry (Poznan Radiocarbon Laboratory, Poznan, Poland) (Kock, Schittek, Wissel, et al., 2019; Schittek et al., 2016). Radiocarbon ages were calibrated to calendar ages (cal. yr BP) using CALIB 7.0.4 (Stuiver et al., 2013) and the Southern Hemisphere (SHCal13) calibration curve (Hogg et al., 2013). Modern radiocarbon ages were calibrated with CALIBomb (Reimer et al., 2004). Age-depth models including confidence intervals were calculated as cubic smoothing splines based on the median of 800 Monte Carlo simulations (MCAgeDepth software, Higuera et al., 2009).

Cellulose extraction followed the CUAM protocol (Wissel et al., 2008). Samples were dispersed with NaOH solution (5%) for 2 hr, washed with deionized water, and sieved at 200- and 1,000-μm mesh width to generate three size classes prior to cellulose extraction. Due to a lack of material within the fraction >1,000 μm and highly correlating signals between the two fractions <200 and 200–1,000 μm (LP: $R^2 = 0.97$, $p < 0.01$; CTP: $R^2 = 0.97$, $p < 0.01$), the fraction 200–1,000 μm was chosen for cellulose extraction for both sites.

3.2. Oxygen Isotope Measurement and Data Processing

Approximately, a 275 μg of freeze-dried cellulose from each sample was weighed in silver capsules. Following crimping, samples were stored for >24 hr in a vacuum drier at 100 °C before measurement. To determine the $^{18}O/^{16}O$ ratio, samples were pyrolyzed at 1,450 °C in a high temperature pyrolysis oven (HT-O, HEKAtech) and measured with a coupled isotope ratio mass spectrometer (Isoprime, GV Instruments).

Isotope data are reported as δ values (‰) following the equation

$$\delta = R_S/R_{St} - 1 \bullet 1000,$$

with R_S as the isotope ratio of the sample ($^{18}O/^{16}O$) and R_{St} as the isotope ratio of the standard. Two international Atomic Energy Agency (IAEA) reference standards IAEA-601 ($\delta^{18}O = 23.14‰$) and IAEA-602 ($\delta^{18}O = 71.28‰$) were used to calibrate laboratory standards and to scale normalize the raw values to the Vienna Standard Mean Ocean Water (VSMOW) scale. Laboratory standards included IAEA-CH6 cellulose powder ($\delta^{18}O = 37.09 \pm 0.09‰$), technical cellulose powders from Merk ($\delta^{18}O = 29.97 \pm 0.08‰$) and Fluka ($\delta^{18}O = 28.84 \pm 0.12‰$), and the in-house standards rice cellulose ($\delta^{18}O = 23.64 \pm 0.15‰$) and peanut cellulose ($\delta^{18}O = 23.93‰ \pm 0.11‰$). The precision of replicate analyses is estimated as <0.25‰.

As the LP record is interspersed with repeated clastic layers (see Kock, Schittek, Lücke, et al., 2019), direct numerical comparison of cushion peatland and other (e.g., SOI) time series was inappropriate. Thus, the averages and standard deviations of the CTP as well as the LP $\delta^{18}O_{cell}$ and the SOI values from Yan et al. (2011) were calculated in the boundaries of the mean ages of the respective 15 peat sections of the LP record (Kock, Schittek, Mächtle, et al., 2019) as base for pairwise statistical analyses (Table S2). Pearson correlation coefficients and the respective p values were calculated using the R software with the "R Stats Package." Additional confidence bands (95%) were calculated by the "Grapher 8" software. Low pass fast Fourier-transform filter (0.005 Hz) was applied within the "Origin" software.

The Online Isotopes in Precipitation Calculator (Bowen, 2020) was used to calculate monthly averaged $\delta^{18}O_{precipitation}$ values (Bowen et al., 2005) for LP and CTP (see Table S1). To estimate potential influences of age uncertainties on the averaging, calculations were repeated by applying (i) the maximum upper and lower ages as well as the (ii) minimum upper and lower ages (Tables S3 and S4).

Due to the discontinuous nature of the LP $\delta^{18}O_{cell}$ record, a locally weighted regression (LOESS Interpolation) with a spline of $f = 0.2$ was performed, using the MatLab code PBUQ after Breecker (2013), to facilitate direct temporal comparison with other records (Montañez et al., 2016).

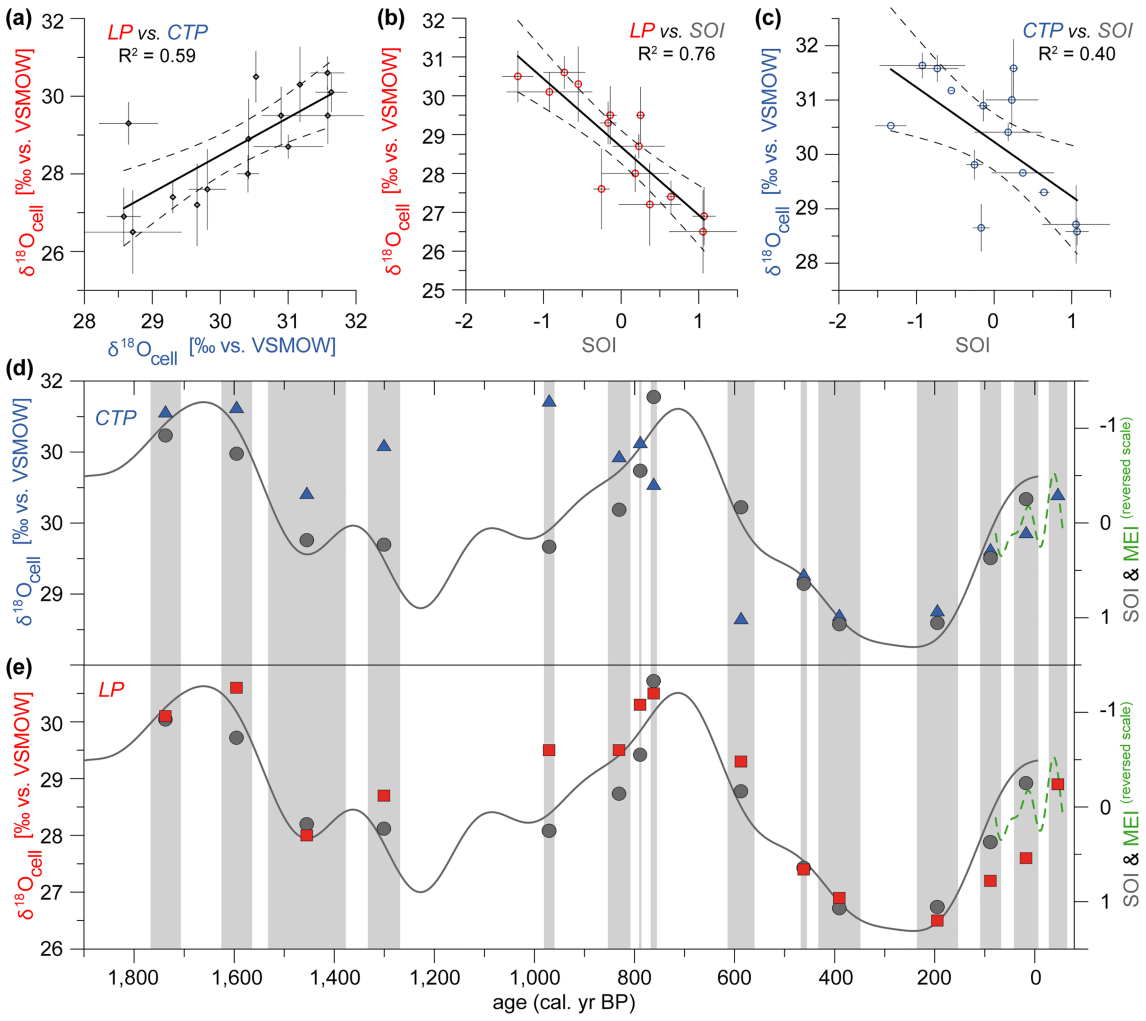

Figure 2. Correlation between mean $\delta^{18}O_{cell}$ LP and CTP values and the SOI. (a) LP $\delta^{18}O_{cell}$ (‰ vs. VSMOW) values against CTP $\delta^{18}O_{cell}$ (‰ vs. VSMOW) values. (b) LP $\delta^{18}O_{cell}$ (‰ vs. VSMOW) values against SOI. (c) CTP $\delta^{18}O_{cell}$ (‰ vs. VSMOW) values against SOI. Given are the standard deviations (horizontal and vertical black lines), the 95% confidence bands (stippled lines) and the coefficients of determination (R^2). (d) CTP $\delta^{18}O_{cell}$ (‰ vs. VSMOW) values (blue triangles) and (e) LP $\delta^{18}O_{cell}$ (‰ vs. VSMOW) values (red squares) compared with the SOI time series (grey line). For comparison, also the mean SOI values (grey circles) used in Figure 2a–c are given. The SOI of Yan et al. (2011) was 0.005 Hz low pass filtered (grey line). Due to the temporal limit of the SOI values at 1950 AD, the multivariate ENSO-index MEI.ext (Wolter & Timlin, 2011) is shown (green line, reverse scaled) to fit to and extend the SOI. The peat sections of LP (grey bands) are indicated for comparison.

4. Results and Discussion

4.1. Variability and Drivers of the $\delta^{18}O_{cell}$ Values on the Puna Plateau During the Last 1,800 Years

Because of the geomorphological setting (see chapter 2), the LP chronology is of discontinuous character with repeated interspersed clastic material between the peat sections. Kock, Schittek, Mächtle, et al. (2019) have presented mean $\delta^{18}O_{cell}$ values for the 15 peat sections described for LP. To allow a direct numerical comparison of both records, the continuous CTP oxygen isotope data were sampled and averaged in the age boundaries of the respective LP peat sections (Table S2). The regression analysis of these section-based $\delta^{18}O_{cell}$ values reveals a high correlation between LP and CTP ($R^2 = 0.59$, $p < 0.01$, Figure 2a). This correlation is even markedly underestimated due to two outliers, that either could be based on the low CTP sample size for the respective LP peat sections (Table S2) or small age-depth model uncertainties (2σ) of the cushion peatland records (Figure S1). Excluding the most extreme of these outliers from analysis would raise the respective R^2 to 0.88 ($p < 0.01$).

In both archives, low (high) $\delta^{18}O_{cell}$ values were interpreted to indicate increased (decreased) moisture availability (Kock, Schittek, Mächtle, et al., 2019; Kock, Schittek, Wissel, et al., 2019), a pattern that can be best explained by SASM-variations connecting increased amounts with depleted $\delta^{18}O$ values of precipitation (Vuille & Werner, 2005). Support for this interpretation came from a negative correlation between $\delta^{18}O_{cell}$ and the thickness of peat layers; hence, peat growth at LP (Kock, Schittek, Mächtle, et al., 2019) and from maximum $\delta^{18}O_{cell}$ values matching with gypsum precipitates at CTP (Kock, Schittek, Wissel, et al., 2019).

The high accordance of both records indeed suggests a shared dominant moisture source during the last 1,800 years. This accordance supports our interpretation of $\delta^{18}O_{cell}$ as recorders of local precipitation availability driven by longer-term dynamics of the SASM-strength. Alternatively, LP could have been influenced by precipitation sourced in the Pacific due to a northward displacement of the SHW during austral winter in the past, although recently such precipitation barely reaches the high-elevated LP catchment area (Kock, Schittek, Mächtle, et al., 2019). Strong precipitation events in the Atacama region of northern Chile in March 2015 were associated with a cutoff cold upper-level low system during unusual warm Pacific surface temperatures (Jordan et al., 2019). These two features seem plausible for increased precipitation in the area of the LP, however, not in the catchment of CTP. If we thus would assume a recurrent impact of the SHW as moisture source or more frequent cutoff events affecting the LP in the past, we would expect higher differences in the $\delta^{18}O_{cell}$ values between the two sites. Calculated monthly $\delta^{18}O_{precipitation}$ values (Bowen et al., 2005) indicate similar values during the summer precipitation season for LP and CTP (Table S1). However, synoptic-scale precipitation events could plausibly trigger the mass movements that are recorded in the LP stratigraphy (Kock, Schittek, Lücke, et al., 2019).

Long-term oxygen isotope oscillations in the Puna between 24° and 27°S during the last 1,800 years seem to be associated with low frequency oscillations described for the atmospheric component of the ENSO-system (SOI). This connection can be drawn from the very high correlations of LP $\delta^{18}O_{cell}$ values with the SOI ($R^2 = 0.76$, $p = 0.04$, Figures 2b and 2d) and the still high correlation between CTP $\delta^{18}O_{cell}$ values and the SOI ($R^2 = 0.40$, $p = 0.01$, Figures 2c and 2e). This observation can be best explained as an indirect relation because during phases of positive (negative) SOI phases, convection and easterly winds over the Amazon Basin are enhanced (reduced) and amplify (reduce) the SASM-strength (e.g. Garreaud & Aceituno, 2001; Liebmann & Mechoso, 2011; Vuille, 1999; Vuille & Werner, 2005). As the initial water vapor $\delta^{18}O$ values are affected by the strength of that upstream convection, $\delta^{18}O_{precipitation}$ values of the Andean highlands are overall more depleted (enriched) during more humid (arid) conditions, although regional differences occur (Insel et al., 2013). This connection was confirmed by using a proxy system model approach, indicating that more than two thirds of $\delta^{18}O$ variability of the Quelccaya ice cap (14°S, Peru) can be accounted for by the ENSO-influence on SASM-activity (Hurley et al., 2019). Building on that previously described connection between ENSO and SASM, the strong coherence between the SOI and our data further supports our argument that the $\delta^{18}O$ values of cushion peatland cellulose values were driven by the SASM-strength. Weaker correlation of the CTP $\delta^{18}O_{cell}$ values with the SOI is noticeable but could be explained by a lower sensitivity to changes in the SASM-expression/strength compared to LP, which is located closer to the Arid Diagonal and in an even more extreme environment. Due to its setting, the LP may be more sensitive towards changes in precipitation supply, which is a possible explanation for the stronger ENSO-dependence compared to CTP in the eastern part of the Puna Plateau.

To investigate the sensitivity of our binning approach (mean values) to age uncertainties of the LP age-depth model, we calculated mean values for the CTP and SOI records based on the minimum, maximum, and mean time span of LPs peat sections (Tables S2, S3, and S4). The resultant, different CTP $\delta^{18}O_{cell}$ and SOI values can be compared to the unmodified LP $\delta^{18}O_{cell}$ values, respectively (Figures S2a and S2b). Between these different averaging intervals, only marginal deviations occur. The results of this sensitivity analysis indicates that uncertainties in the leading age model of LP do not affect the high correlation between the LP $\delta^{18}O_{cell}$ values and the SOI (Figure S2a) and also do not decrease the correlation between the CTP $\delta^{18}O_{cell}$ values and the SOI (Figure S2b) significantly.

4.2. Multi-Centennial SASM-Dynamics

During the last 1,800 years, the $\delta^{18}O_{cell}$ records of LP and CTP reveal multi-centennial changes in moisture conditions in the Puna Plateau (24–27°S). Increased SASM-strength, and thus, precipitation amounts are

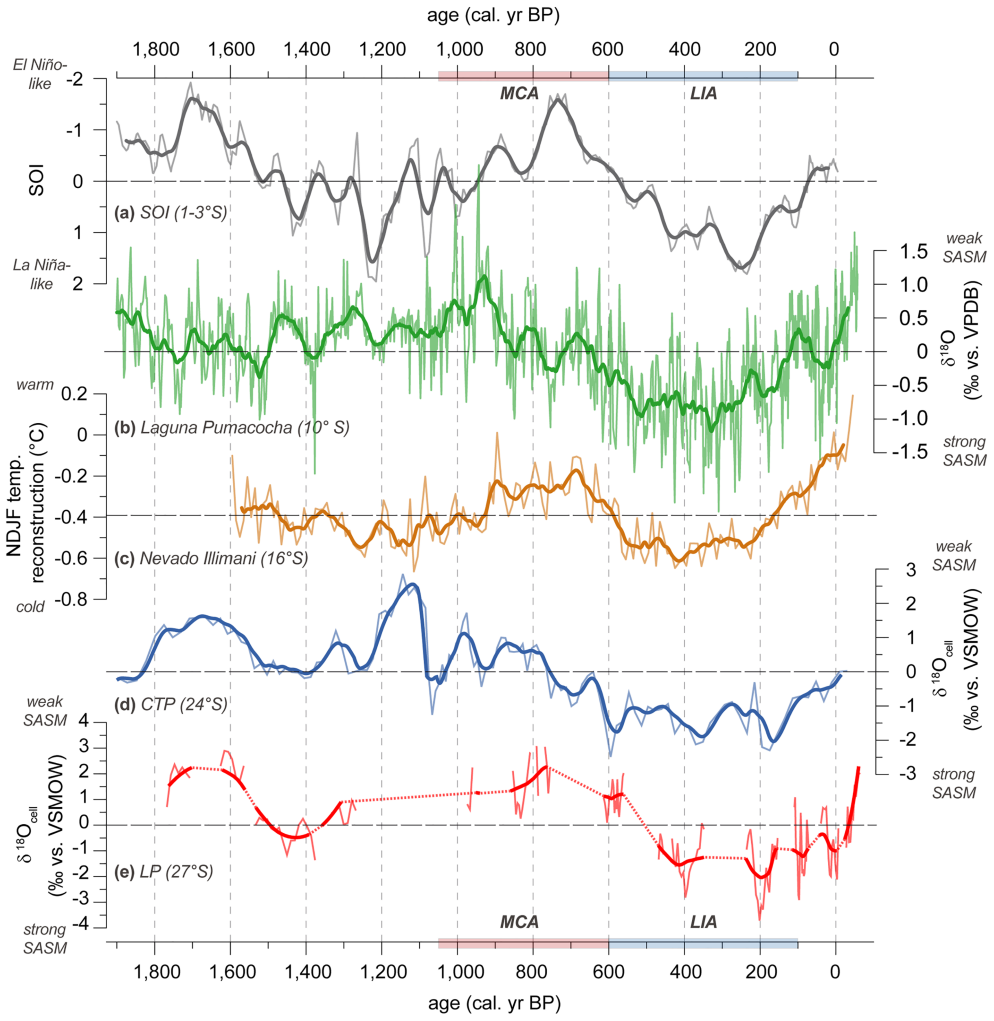

Figure 3. Paleoclimate comparison of CTP and LP. (a) Reverse-scaled Southern Oscillation Index (SOI) (1–3°S; Yan et al., 2011). (b) $\delta^{18}O$ (‰ vs. VPDB) of Laguna Pumacocha (10°S, Peru; Bird et al., 2011). (c) NDJF temperature anomalies (°C) of Nevado Illimani reconstructed from ammonium concentrations (16°S, Bolivia; Kellerhals et al., 2010). (d) $\delta^{18}O_{cell}$ (‰ vs. VSMOW) of the Cerro Tuzgle peatland (24°S, Argentina; Kock, Schittek, Wissel, et al., 2019). (e) $\delta^{18}O_{cell}$ (‰ vs. VSMOW) of the Lagunillas peatland (27°S, Chile; Kock, Schittek, Mächtle, et al., 2019), bold and dotted lines indicate the LOESS interpolation ($f = 0.2$) based on Montañez et al. (2016). Note that all values are displayed as normalized values. Additionally, the values of (a–d) were annualized (original data in transparent colors) and smoothed using a 51-year running window (bold lines). The Medieval Climate Anomaly (MCA) is indicated in red and the Little Ice Age (LIA) in blue.

indicated for multi-centennial phases between 1,530 to 1,270 cal. yr BP and during the pronounced Little Ice Age (LIA) period between 470 to 70 cal. yr BP. For the time before 1,550 cal. yr BP and the period between 1,280 and 470 cal. yr BP, a reduced SASM-intensity with decreased precipitation amounts is indicated accordingly. Here we compare these observed SASM-dynamics with other paleoclimatic SASM-records (Figure 3).

The SOI reconstruction (Figure 3a) indicates remarkable correspondence with the cushion peatland $\delta^{18}O_{cell}$ records (CTP: Figure 3d, LP: Figure 3e) on multi-centennial timescales. Today, wet summers in the Puna Plateau are associated with a La Niña-related cooling of the tropical Pacific, a shrinking of the tropical troposphere, and thus, enhanced easterly flow (equal to extensive SASM) over the Andean highlands as a response to the changes in meridional baroclinicity between tropical and subtropical latitudes (Garreaud et al., 2003). This (indirect) coupling between ENSO-like dynamics, respectively, SASM-strength and the cushion peatland $\delta^{18}O_{cell}$ values is also evident from the high accordance with the record of Ammonium

concentration of the Nevado Illimani reflecting November to February-temperature changes of the Amazon Basin (Figure 3c; Kellerhals et al., 2010). Cold air incursions, especially during austral spring, tend to positively correlate with SASM-precipitation by enhancing forced ascent in a thermodynamically primed atmosphere, thus leading to enhanced SASM-strength with decreasing temperatures (e.g., Hurley et al., 2015; Raia & Cavalcanti, 2008).

Compared to the conventional interpretations about ENSO-conditions during the last 2,000 years, our findings seem to differ at first glance. Whereas we observe drier conditions (reduced SASM) and a negative SOI-phase (El Niño-like) for the Medieval Climate Anomaly, common interpretations associate the Medieval Climate Anomaly with La Niña-like conditions, while the LIA is often associated with El Niño-like conditions (e.g., Cobb et al., 2003; Denniston et al., 2015; Mann et al., 2009). However, interpretations are still subject to scientific discussions, and even contrary results have been published (Conroy et al., 2008; Lüning et al., 2019; Moy et al., 2002; Martel-Cea et al., 2016; Rustic et al., 2015; Tan et al., 2019; Yan et al., 2011; see Figure S3). Barr et al. (2019) stated that differences in interpretation arise due to heterogenic relationship between terrestrial hydroclimate proxies, oceanic sea surface temperature proxies, and theoretical and physical models of predicted responses to global temperature changes. Other elements of uncertainty are modified ENSO-signals with specific regional responses that sometimes lead to complete reverse effects in a close area. The transition from one extreme response to the other is complex and not uniform and depends on the region and the season analyzed (Vuille et al., 2000). Recently, Schneider et al. (2018) even recommended a reinvestigation of existing proxy-climate relationships to improve Paleo-ENSO reconstructions, as not all ENSO-records, for example Laguna Pallcacocha, seem to be equally qualified. Irrespective of this question, the relation between our $\delta^{18}O$ proxy records and SASM-forcing remains valid and may foster further discussions.

As indicated by the high correlations between the averaged peat sections $\delta^{18}O_{cell}$ LP and CTP values (Section 4.1), the records of CTP (Figure 3d) and LP (Figure 3e) reveal a high conformity in their temporal development. The depicted multi-centennial changes of $\delta^{18}O_{cell}$ values can partly be found in different archives of the northern central Andes, indicating also the dependency on the SASM-system. However, contrary to the good match between SOI and Illimani temperature reconstruction, SASM-records from the northern central Andes seem to reveal deviations. For example, $\delta^{18}O$ values of Laguna Pumacocha (~10° S, Bird et al., 2011, Figure 3b) show comparable results only during the last 750 years, thus the LIA period, but markedly deviate before 700 cal. yr BP, partly almost showing the opposite development. Other $\delta^{18}O$ records like from Huagapo Cave (~11°S, Kanner et al., 2013) or Quelccaya ice cap (~13°S, Thompson et al., 2013) show comparable behavior (not shown). Despite their relative proximity, the records of northern central Andes differ surprisingly strong from each other which might indicate a bias due to different types of geoarchives or special regional features.

Reasons for the differences between the northern and southern central Andes, considering unaltered seasonal precipitation regimes, might be linked to changes in atmospheric overturning circulation systems. Latitudinal shifts of the precipitation regime evolving from mid- and upper tropospheric wind anomalies can lead to different (out of phase) SASM-modes as described by Vuille and Keimig (2004). Increased convection and tropical precipitation in the Andean highlands between 10 and 20°S is present during a northern mode, while increased precipitation amounts in the eastern Cordillera between 15°S and 22°S prevail during a northeastern SASM-mode (Vuille & Keimig, 2004). Contrary, a southward displacement of the Bolivian High as well as Rossby wave dispersion derived from the Southern Hemisphere extratropics represents a southern SASM-mode, leading to enhanced precipitation in the southern central Andes between 20°S and 30°S (Vuille & Keimig, 2004). Another potential factor explaining regional differences between the northern and southern central Andes is the influence of the South Atlantic convergence zone (SACZ), which is characterized by a dipole-like pattern with the SALLJ, and occurs with frequencies from intraseasonal to interdecadal timescales (Cerne & Vera, 2011; Díaz & Aceituno, 2003; Liebmann & Mechoso, 2011). This SALLJ/SACZ dipole is characterized by reduced (enhanced) SACZ-activity and enhanced (reduced) convection in the sub-tropical plains along the Andes of NW Argentina due to an intensified (suppressed) SALLJ (Liebmann & Mechoso, 2011). A strengthening of the SALLJ can be associated with the transport of massive amounts of moisture from the Amazon Basin into the sub-tropics and is linked to short-term extreme precipitation events (Salio et al., 2007). Thus, reduced activity of the SACZ for longer periods could lead to a less

distracted SALLJ, enhanced mesoscale convective activity along plains of the Eastern Cordillera, and therefore increased precipitation amounts in the southern central Andes. Thus, the interaction of several driving forces (e.g., out-of-phase SASM-modes, SACZ/SALLJ dipole, and location of the ITCZ) can lead to a temporal modulation in the SASM response in the northern and southern central Andes and reveal the need for further investigations based on the research presented here.

5. Conclusions

The $\delta^{18}O_{cell}$ cushion peatland records CTP and LP (24–27°S) reveal multi-centennial changes of the SASM-strength since 1,800 cal. yr BP on the Puna Plateau. As the two peatland archives reveal a high conformity in their temporal development, we conclude that the SASM is the main forcing factor for changes in moisture conditions and exclude a temporal dominant forcing of the SHW. The conspicuous high correlation between the centennial scale SOI and our records indicates the teleconnection between the ENSO and the SASM-system and supports our interpretation of the CTP and LP $\delta^{18}O_{cell}$ values. Good conformity of our records with temperature reconstructions of the Amazon Basin, the source region for the SALLJ, further supports the interpretation of SASM-related precipitation changes in the study area. Thus, we can describe late Holocene fluctuations of SASM-strength with increased monsoonal precipitation from 1,530 to 1,270 cal. yr BP and from 470 to 70 cal. yr BP, while reduced monsoonal precipitation prevailed from 1,750 to 1,550 cal. yr BP, 1,200 to 960 cal. yr BP, and since 130 cal. yr BP.

In contrast to the conformity between our SASM-records and the high accordance with SOI and temperature reconstructions of the Amazon Basin, comparisons with SASM-sensitive speleothem, lake, and ice records of the northern central Andes reveal remarkable deviations, especially before 750 cal. yr BP. The reasons for these deviations can be manifold, but presumably are linked to changes in overturning circulation systems, like out of phase-SASM modes or a reduced SACZ activity.

To exclude bias due to differences in archive types as potential reason for spatial and temporal discrepancy in SASM-records and to further elaborate on regionally different SASM-expressions, further cushion peatland isotope studies in the central Andes are needed.

Acknowledgments
Data are available from the National Oceanic and Atmospheric Administration (NOAA) Paleoclimate database (LP: https://www.ncdc.noaa.gov/paleo-search/study/26950; CTP: https://www.ncdc.noaa.gov/paleo-search/study/27270). We gratefully acknowledge support from the German Science Foundation (DFG) priority research program SPP-1803 "EarthShape: Earth Surface Shaping by Biota" (Grants Ma 4504/1-1 to BM and Schi 1366/1-1 to KS) and to FS (Scha 14-1/2). We further acknowledge funding from the German Federal Ministry for Education and Research to KS (ARG 06/009), the National Geographic Society to KS (Grant 8030-06), the National University of Jujuy to LL (SeCTER), and from the German Academic Exchange Service (DAAD) PROMOS—scholarship for thesis preparation 2015 to SK. We are grateful to the Chilean National Park Service (CONAF) for providing access to the sites and further onsite support. Furthermore, we sincerely thank Eugenia de Porras, Gabriel Cortés, Fabio Flores, Gonzalo Torres, and Leandro Rojo for all the support during the different field campaigns and to Prof Dr Barbara Ruthsatz for her advice on the ecology of cushion peatlands. This work is dedicated to our colleague Heike Zimmermann who passed away too early.

References

Alfaro-Sánchez, R., Nguyen, H., Klesse, S., Hudson, A., Belmecheri, S., Köse, N., et al. (2018). Climatic and volcanic forcing of tropical belt northern boundary over the past 800 years. *Nature Geoscience*, *11*(12), 933–938. https://doi.org/10.1038/s41561-018-0242-1

Barr, C., Tibby, J., Leng, M. J., Tyler, J. J., Henderson, A. C. G., Overpeck, J. T., et al. (2019). Holocene El Niño–southern Oscillation variability reflected in subtropical Australian precipitation. *Scientific Reports*, *9*(1), 1–9. https://doi.org/10.1038/s41598-019-38626-3

Bird, B. W., Abbott, M. B., Vuille, M., Rodbell, D. T., Stansell, N. D., & Rosenmeier, M. F. (2011). A 2,300-year-long annually resolved record of the South American summer monsoon from the Peruvian Andes. *Proceedings of the National Academy of Sciences*, *108*, 8583–8588. https://doi.org/10.1073/pnas.1003719108

Bowen, G. J. (2020). The online isotopes in precipitation calculator, version 3.1. http://www.waterisotopes.org.

Bowen, G. J., Wassenaar, L. I., & Hobson, K. A. (2005). Global application of stable hydrogen and oxygen isotopes to wildlife forensics. *Oecologia*, *143*(3), 337–348. https://doi.org/10.1007/s00442-004-1813-y

Breecker, D. O. (2013). Quantifying and understanding the uncertainty of atmospheric CO_2 concentrations determined from calcic paleosols. *Geochemistry, Geophysics, Geosystems*, *14*, 3210–3220. https://doi.org/10.1002/ggge.20189

Cerne, S. B., & Vera, C. S. (2011). Influence of the intraseasonal variability on heat waves in subtropical South America. *Climate Dynamics*, *36*(11-12), 2265–2277. https://doi.org/10.1007/s00382-010-0812-4

Cobb, K. M., Charles, C. D., Cheng, H., & Edwards, R. L. (2003). El Niño/Southern Oscillation and tropical Pacific climate during the last millennium. *Nature*, *424*(6946), 271–276. https://doi.org/10.1038/nature01779

Conroy, J. L., Overpeck, J. T., Cole, J. E., Shanahan, T. M., & Steinitz-Kannan, M. (2008). Holocene changes in eastern tropical Pacific climate inferred from a Galápagos lake sediment record. *Quaternary Science Reviews*, *27*(11-12), 1166–1180. https://doi.org/10.1016/j.quascirev.2008.02.015

de Porras, M. E., & Maldonado, A. (2016). Metodologías y avances de la palinología del Cuaternario tardío a lo largo de la Diagonal Árida Sudamericana. *Publicación Electrónica de la Asociación Paleontológica Argentina*, *18*(2), 18–38. https://doi.org/10.5710/PEPAPA.08.07.2018.255

Denniston, R. F., Villarini, G., Gonzales, A. N., Wyrwoll, K. H., Polyak, V. J., Ummenhofer, C. C., et al. (2015). Extreme rainfall activity in the Australian tropics reflects changes in the El Niño/Southern Oscillation over the last two millennia. *Proceedings of the National Academy of Sciences*, *112*(15), 4576–4581. https://doi.org/10.1073/pnas.1422270112

Díaz, A., & Aceituno, P. (2003). Atmospheric circulation anomalies during episodes of enhanced and reduced convective cloudiness over Uruguay. *Journal of Climate*, *16*(19), 3171–3185. https://doi.org/10.1175/1520-0442(2003)016<3171:ACADEO>2.0.CO;2

Engel, Z., Skrzypek, G., Chuman, T., Šefrna, L., & Mihaljevič, M. (2014). Climate in the western cordillera of the central Andes over the last 4300 years. *Quaternary Science Reviews*, *99*, 60–77. https://doi.org/10.1016/j.quascirev.2014.06.019

Fick, S. E., & Hijmans, R. J. (2017). WorldClim 2: New 1-km spatial resolution climate surfaces for global land areas. *International Journal of Climatology*, *37*(12), 4302–4315. https://doi.org/10.1002/joc.5086

Garreaud, R. D. (2000). Intraseasonal variability of moisture and rainfall over the South American Altiplano. *Monthly Weather Review*, *128*(9), 3337–3346. https://doi.org/10.1175/1520-0493(2000)128<3337:IVOMAR>2.0.CO;2

Garreaud, R. D., & Aceituno, P. (2001). Interannual rainfall variability over the South American Altiplano. *Journal of Climate*, *14*(12), 2779–2789. https://doi.org/10.1175/1520-0442(2001)014<2779:IRVOTS>2.0.CO;2

Garreaud, R. D., Vuille, M., & Clement, A. C. (2003). The climate of the Altiplano: Observed current conditions and mechanisms of past changes. *Palaeogeography, Palaeoclimatology, Palaeoecology*, *194*(1-3), 5–22. https://doi.org/10.1016/S0031-0182(03)00269-4

Gergis, J., Braganza, K., Fowler, A., Mooney, S., & Risbey, J. (2006). Reconstructing El Niño–Southern Oscillation (ENSO) from high-resolution palaeoarchives. *Journal of Quaternary Science*, *21*(7), 707–722. https://doi.org/10.1002/jqs.1070

Hardy, D. R., Vuille, M., & Bradley, R. S. (2003). Variability of snow accumulation and isotopic composition on Nevado Sajama, Bolivia. *Journal of Geophysical Research*, *108*(D22), 4693. https://doi.org/10.1029/2003JD003623

Henke, L. M. K., Lambert, F. H., & Charman, D. J. (2017). Was the Little Ice Age more or less El Niño-like than the Medieval Climate Anomaly? Evidence from hydrologicaland temperature proxy data. *Climate of the Past*, *13*, 267–301. https://doi.org/10.5194/cp-13-267-2017

Higuera, P. E., Brubaker, L. B., Anderson, P. M., Sheng Hu, F., & Brown, T. A. (2009). Vegetation mediated the impacts of postglacial climate change on fire regimes in the south-central Brooks Range, Alaska. *Ecological Monographs*, *79*(2), 201–219. https://doi.org/10.1890/07-2019.1

Hogg, A. G., Hua, Q., Blackwell, P. G., Niu, M., Buck, C. E., Guilderson, T. P., et al. (2013). SHCAL13 southern hemisphere calibration, 0-50,000 years cal BP. *Radiocarbon*, *55*(4), 1889–1903. https://doi.org/10.2458/azu_js_rc.55.16783

Hurley, J. V., Vuille, M., & Hardy, D. R. (2019). On the interpretation of the ENSO signal embedded in the stable isotopic composition of Quelccaya Ice Cap, Peru. *Journal of Geophysical Research: Atmospheres*, *124*, 131–145. https://doi.org/10.1029/2018JD029064

Hurley, J. V., Vuille, M., Hardy, D. R., Burns, S. J., & Thompson, L. G. (2015). Cold air incursions, $\delta^{18}O$ variability, and monsoon dynamics associated with snow days at Quelccaya Ice Cap, Peru. *Journal of Geophysical Research: Atmospheres*, *120*, 7467–7487. https://doi.org/10.1002/2015JD023323

Insel, N., Poulsen, C. J., Sturm, C., & Ehlers, T. A. (2013). Climate controls on Andean precipitation $\delta^{18}O$ interannual variability. *Journal of Geophysical Research: Atmospheres*, *118*, 9721–9742. https://doi.org/10.1002/jgrd.50619

Jordan, T. E., Herrera, L. C., Godfrey, L. V., Colucci, S. J., Gamboa, P. C., Urrutia, M. J., et al. (2019). Isotopic characteristics and paleo-climate implications of the extreme precipitation event of March 2015 in northern Chile. *Andean Geology*, *46*(1), 1–31. https://doi.org/10.5027/andgeoV46n1-3087

Kanner, L. C., Burns, S. J., Cheng, H., Edwards, R. L., & Vuille, M. (2013). High-resolution variability of the South American summer monsoon over the last seven millennia: Insights from a speleothem record from the central Peruvian Andes. *Quaternary Science Reviews*, *75*, 1–10. https://doi.org/10.1016/j.quascirev.2013.05.008

Kellerhals, T., Brütsch, S., Sigl, M., Knüsel, S., Gäggeler, H. W., & Schwikowski, M. (2010). Ammonium concentration in ice cores: A new proxy for regional temperature reconstruction? *Journal of Geophysical Research*, *115*, D16123. https://doi.org/10.1029/2009JD012603

Kock, S. T., Schittek, K., Lücke, A., Maldonado, A., & Mächtle, B. (2019). Geomorphodynamics of the western Chilean central Andes (27°S) during the last 1800 cal. yr BP as recorded in a high-Andean cushion peatland. *Zeitschrift für Geomorphologie, Supplementary Issues*, *62*(2), 183–205. https://doi.org/10.1127/zfg_suppl/2019/0537

Kock, S. T., Schittek, K., Mächtle, B., Wissel, H., Maldonado, A., & Lücke, A. (2019). Late Holocene environmental changes reconstructed from stable isotope and geochemical records from a cushion-plant peatland in the Chilean central Andes (27°S). *Journal of Quaternary Science*, *34*(2), 153–164. https://doi.org/10.1002/jqs.3088

Kock, S. T., Schittek, K., Wissel, H., Vos, H., Ohlendorf, C., Schäbitz, F., et al. (2019). Stable oxygen isotope records ($\delta^{18}O$) of a high-Andean cushion peatland in NW Argentina (24°S) imply South American Summer Monsoon related moisture changes during the Late Holocene. *Frontiers in Earth Science*, *7*, 45. https://doi.org/10.3389/feart.2019.00045

Liebmann, B., & Mechoso, C. R. (2011). The south american monsoon system. In C.-P. Chang, Y. Ding, N.-C. Lau, R. H. Johnson, B. Wang, & T. Yasunari (Eds.), *The global monsoon system research and forecast* (pp. 137–157). Singapore: World of Scientific. https://doi.org/10.1142/9789814343411_0009

Lüning, S., Gałka, M., Bamonte, F. P., Rodríguez, F. G., & Vahrenholt, F. (2019). The Medieval Climate Anomaly in South America. *Quaternary International*, *508*, 70–87. https://doi.org/10.1016/j.quaint.2018.10.041

MacDonald, G. M., & Case, R. A. (2005). Variations in the Pacific Decadal Oscillation over the past millennium. *Geophysical Research Letters*, *32*, L08703. https://doi.org/10.1029/2005GL022478

Mann, M. E., Zhang, Z., Rutherford, S., Bradley, R. S., Hughes, M. K., Shindell, D., et al. (2009). Global signatures and dynamical origins of the Little Ice Age and Medieval Climate Anomaly. *Science*, *326*(5957), 1256–1260. https://doi.org/10.1126/science.1177303

Marengo, J. A., Liebmann, B., Grimm, A. M., Misra, V., Silva Dias, P. L., Cavalcanti, I. F. A., et al. (2012). Recent developments on the South American monsoon system. *International Journal of Climatology*, *32*(1), 1–21. https://doi.org/10.1002/joc.2254

Martel-Cea, A., Maldonado, A., Grosjean, M., Alvial, I., de Jong, R., Fritz, S. C., & von Gunten, L. (2016). Late Holocene environmental changes as recorded in the sediments of high Andean Laguna Chepical, Central Chile (32°S; 3050 m asl). *Palaeogeography, Palaeoclimatology, Palaeoecology*, *461*, 44–54. https://doi.org/10.1016/j.palaeo.2016.08.003

Montañez, I. P., McElwain, J. C., Poulsen, C. J., White, J. D., DiMichele, W. A., Wilson, J. P., et al. (2016). Climate, ρCO_2 and terrestrial carbon cycle linkages during late Palaeozoic glacial–interglacial cycles. *Nature Geoscience*, *9*(11), 824–828. https://doi.org/10.1038/NGEO2822

Moy, C. M., Seltzer, G. O., Rodbell, D. T., & Anderson, D. M. (2002). Variability of El Niño/Southern Oscillation activity at millennial timescales during the Holocene epoch. *Nature*, *420*(6912), 162. https://doi.org/10.1038/nature01194

Norini, G., Cogliati, S., Baez, W., Arnosio, M., Bustos, E., Viramonte, J., & Groppelli, G. (2014). The geological and structural evolution of the Cerro Tuzgle Quaternary stratovolcano in the back-arc region of the Central Andes, Argentina. *Journal of Volcanology and Geothermal Research*, *285*, 214–228. https://doi.org/10.1016/j.jvolgeores.2014.08.023

Raia, A., & Cavalcanti, I. F. A. (2008). The life cycle of the South American monsoon system. *Journal of Climate*, *21*(23), 6227–6246. https://doi.org/10.1175/2008JCLI2249.1

Reimer, P. J., Brown, T. A., & Reimer, R. W. (2004). Discussion: reporting and calibration of post-bomb ^{14}C data. *Radiocarbon*, *46*(3), 1299–1304. https://doi.org/10.1017/S0033822200033154

Rustic, G. T., Koutavas, A., Marchitto, T. M., & Linsley, B. K. (2015). Dynamical excitation of the tropical Pacific Ocean and ENSO variability by Little Ice Age cooling. *Science*, *350*(6267), 1537–1541. https://doi.org/10.1126/science.aac9937

Salio, P., Nicolini, M., & Zipser, E. J. (2007). Mesoscale convective systems over southeastern South America and their relationship with the South American low-level jet. *Monthly Weather Review*, *135*(4), 1290–1309. https://doi.org/10.1175/MWR3305.1

Schittek, K. (2014). *Cushion peatlands in the high Andes of Northwest Argentina as archives for palaeoenvironmental research*. Stuttgart: J. Cramer in der Gebrüder Borntraeger Verlagsbuchhandlung.

Schittek, K., Forbriger, M., Berg, D., Hense, J., Schäbitz, F., & Eitel, B. (2018). Last millennial environmental dynamics in the western Peruvian Andes inferred from the development of a cushion-plant peat hillock. *Perspectives in Plant Ecology, Evolution and Systematics*, *30*, 115–124. https://doi.org/10.1016/j.ppees.2017.09.002

Schittek, K., Forbriger, M., Mächtle, B., Schäbitz, F., Wennrich, V., Reindel, M., & Eitel, B. (2015). Holocene environmental changes in the highlands of the southern Peruvian Andes (14°S) and their impact on pre-Columbian cultures. *Climate of the Past*, *11*(1), 27–44. https://doi.org/10.5194/cp-11-27-2015

Schittek, K., Kock, S. T., Lücke, A., Ohlendorf, C., Kulemeyer, J. J., Lupo, L. C., & Schäbitz, F. (2016). A high-altitude peatland record of environmental changes in the NW Argentine Andes (24°S) over the last 2100 years. *Climate of the Past*, *12*(5), 1165–1180. https://doi.org/10.5194/cp-12-1165-2016

Schneider, T., Hampel, H., Mosquera, P. V., Tylmann, W., & Grosjean, M. (2018). Paleo-ENSO revisited: Ecuadorian Lake Pallcacocha does not reveal a conclusive El Niño signal. *Global and Planetary Change*, *168*, 54–66. https://doi.org/10.1016/j.gloplacha.2018.06.004

Stuiver, M., Reimer, P. J., & Reimer, R. W. (2013). Calib 7.0, Radiocarbon calibration program, available at: http://calib.org/calib/download/calib704.zip.

Tan, L., Shen, C. C., Löwemark, L., Chawchai, S., Edwards, R. L., Cai, Y., et al. (2019). Rainfall variations in central Indo-Pacific over the past 2,700 y. *Proceedings of the National Academy of Sciences*, *116*(35), 17,201–17,206. https://doi.org/10.1073/pnas.1903167116

The International Atomic Energy Agency/World Meteorological Organization (2015). Data from: Global Network of Isotopes in Precipitation., GNIP Database (2015), available at: https://nucleus.iaea.org/wiser/index.php.

Thompson, L. G., Mosley-Thompson, E., Davis, M. E., Zagorodnov, V. S., Howat, I. M., Mikhalenko, V. N., & Lin, P.-N. (2013). Annually resolved ice core records of tropical climate variability over the past ~1800 years. *Science*, *340*(6135), 945–950. https://doi.org/10.1126/science.1234210

Trenberth, K. E. (1997). The definition of El Niño. *Bulletin of the American Meteorological Society*, *78*(12), 2771–2778. https://doi.org/10.1175/1520-0477(1997)078<2771:TDOENO>2.0.CO;2

Vera, C., Higgins, W., Amador, J., Ambrizzi, T., Garreaud, R., Gochis, D., et al. (2006). Toward a unified view of the American Monsoon systems. *Journal of Climate*, *19*(20), 4977–5000. https://doi.org/10.1175/JCLI3896.1

Vuille, M. (1999). Atmospheric circulation over the Bolivian Altiplano during dry and wet periods and extreme phases of the Southern Oscillation. *International Journal of Climatology*, *19*(14), 1579–1600. https://doi.org/10.1002/(SICI)1097-0088(19991130)19:14<1579::AID-JOC441>3.0.CO;2-N

Vuille, M., & Ammann, C. (1997). Regional snowfall patterns in the high, arid Andes. *Climatic Change*, *36*(3-4), 413–423. https://doi.org/10.1023/A:1005330802974

Vuille, M., Bradley, R. S., & Keimig, F. (2000). Climate variability in the Andes of Ecuador and its relation to Tropical Pacific and Atlantic Sea Surface Temperature Anomalies. *Journal of Geophysical Research*, *105*(D10), 12,447–12,460. https://doi.org/10.1029/2000JD900134

Vuille, M., Burns, S. J., Taylor, B. L., Cruz, F. W., Bird, B. W., Abbott, M. B., et al. (2012). A review of the South American monsoon history as recorded in stable isotopic proxies over the past two millennia. *Climate of the Past*, *8*(4), 1309–1321. https://doi.org/10.5194/cp-8-1309-2012

Vuille, M., & Keimig, F. (2004). Interannual variability of summertime convective cloudiness and precipitation in the central Andes derived from ISCCP-B3 Data. *Journal of Climate*, *17*(17), 3334–3348. https://doi.org/10.1175/1520-0442(2004)017<3334:IVOSCC>2.0.CO;2

Vuille, M., & Werner, M. (2005). Stable isotopes in precipitation recording South American summer monsoon and ENSO variability: Observations and model results. *Climate Dynamics*, *25*(4), 401–412. https://doi.org/10.1007/s00382-005-0049-9

Werner, D. J. (1974). Landschaftsökologische Untersuchungen in der argentinischen Puna. In C. Rathjens, & M. Born (Eds.), *Tagungsbericht und Wissenschaftliche Abhandlungen, Deutscher Geographentag Kassel 1973* (pp. 508–528). Kassel: F. Steiner Verlag.

Wissel, H., Mayr, C., & Lücke, A. (2008). A new approach for the isolation of cellulose from aquatic plant tissue and freshwater sediments for stable isotope analysis. *Organic Geochemistry*, *39*(11), 1545–1561. https://doi.org/10.1016/j.orggeochem.2008.07.014

Wolter, K., & Timlin, M. S. (2011). El Niño/Southern Oscillation behaviour since 1871 as diagnosed in an extended multivariate ENSO index (MEI.ext). *International Journal of Climatology*, *31*(7), 1074–1087. https://doi.org/10.1002/joc.2336

Yan, H., Sun, L., Wang, Y., Huang, W., Qiu, S., & Yang, C. (2011). A record of the Southern Oscillation Index for the past 2,000 years from precipitation proxies. *Nature Geoscience*, *4*(9), 611. https://doi.org/10.1038/NGEO1231